Received: 30 April 2022 | Revised: 4 July 2022 | Accepted: 13 July 2022 | Published online: 16 July 2022

RESEARCH ARTICLE

Journal of Computational and Cognitive Engineering
2024, Vol. 3(1) 43–57
DOI: 10.47852/bonviewJCCE2202236

BON VIEW PUBLISHING

COVID-19 Outbreak with Fuzzy Uncertainties: A Mathematical Perspective

Prasenjit Mahato[1], **Sanat Kumar Mahato**[1,*] and **Subhashis Das**[1]

[1]*Department of Mathematics, Sidho-Kanho-Birsha University, India*

Abstract: In this article, we design a mathematical SEQAIMR (susceptible, exposed, quarantined, asymptomatic, symptomatic, isolated, recovered) epidemic model and investigate the nature of the system. We transform the crisp model into the fuzzy model. All the biological parameters are treated as triangular fuzzy numbers (TFNs). With the help of utility function method, the fuzzy model is defuzzified. We use the MATLAB codes to solve the system of equations and to predict different situations under different values of the control parameters. Lastly, optimal control for COVID-19 disease is explained.

Keywords: COVID-19 virus, triangular fuzzy number, utility function method, optimal control

1. Introduction

The model formulation of infectious disease is the most important tool to fathom of its epidemiological prototypes. It helps us to take suitable measure to control its severity. Recently, it is a great threat throughout the world from COVID-19. Coronavirus disease is exponentially (Velavan & Meyer, 2020; Wu & McGoogan, 2020) growing, and patients in main land China were detected with COVID-19. The authority of China promptly initiated the radical measure to control the outbreak (Chakraborty & Ghosh, 2020; Chen et al., 2020; He et al., 2020; Kumar et al., 2020; Nadim et al., 2021; Nesteruk, 2020; Tiwari, 2020; Wu et al., 2020). In spite of radical measure, it is shaped an epidemic and China became the epicenter. World Health Organization described coronavirus as family of virus. Respiratory droplets and contact transmission are the important way for transmission of coronavirus. Its incubation period is 2–14 days (Yang & Wang, 2020). Generally, COVID-19 patients suffer from high fever, sneeze, dry cough, tiredness, runny nose, and lung penetration. This infectious disease is spread all over the world by human dynamism. India, USA, and Europe become the epicenter of coronavirus. Shared surfaces are a serious risky. Because the coronavirus may alive or it may remain infectious from 2 h up to 1 week on different kind of metals such as aluminum, metal, wood, silicon, steel, glass, rubber, and paper (Kampf et al., 2020). Giordano et al. (2020) explained a mathematical model for coronavirus disease and described the combining both strict lockdown and testing can control the severity of infectious coronavirus disease within human. Verity et al. (2020) explained a model-based analysis. Khajanchi and Sarkar (2020) investigated the transmission dynamics and forecasting SARS-CoV-2 virus for many states on their mathematical model. Khajanchi et al. (2020) developed a new mathematical model for describing the transmission dynamics in different states in India. Pal et al. (2020) designed the SEQIR epidemic model. They used data-driven epidemiological parameter for spreading in India (Pal et al., 2020). A SEIR model was discussed by Read et al. (2021) on real data. They found basic reproduction ratio 3.1 (Read et al., 2021). A SIR model was developed by Volpert et al. (2020). They explained for restriction the increasing of coronavirus disease through initiating firm quarantine procedure. The mathematical model on infection kinetics was proposed by Liang (2020). They analyzed for COVID-19, SARS, and MARS on his research work.

In this work, we have explained SEQAIMR (susceptible, exposed, quarantined, asymptomatic, symptomatic, isolated, recovered) model in fuzzy environment. We have considered the imprecise parameter as triangular fuzzy numbers (TFNs). These TFNs are more easy to use, more intuitive, and helpful for raising delegation and information processing in fuzzy nature. We have defuzzified our proposed model using utility function method (UFM). We use uncertainty for the associated parameters uncertain to form more realistic model. So, we may use the uncertain interval-valued parameter. It may help to inform a real-world mathematical system. Zadeh (1965) first used the uncertainty in his mathematical deduction. Panja et al. (2017) used the fuzzy in his Cholera epidemic model. Researchers paid attention to investigate their infectious disease models in imprecise environments (Lahrouz et al., 2011; Imai et al., 2020; Senapati et al., 2021; Das et al., 2022; Nandi et al., 2018; Cai et al., 2017; Chang et al., 2017, Mahato et al., 2022). Verma et al. (2019) used uncertainty in his outbreak of Ebola virus fuzzy epidemic model in Africa. They assumed fuzzy value of susceptible population and also reproduction number.

This article is organized as follows: We study some preliminaries in Section 2. We investigate both the model calibration crisp model and fuzzy model and their assumption in Section 3. Boundedness of the system, equilibria, and stability analysis are performed in the theoretical study portion in Section 4. Optimal control for COVID-19 disease is described in Section 5. Some numerical examples are represented in Section 6. Lastly, conclusions are presented in Section 7.

*Corresponding author: Sanat Kumar Mahato, Department of Mathematics, Sidho-Kanho-Birsha University, India. Email: sanatkr_mahato.math@skbu.ac.in

2. Preliminaries

We introduce some preliminaries to develop the mathematical model. Useful definitions are as follows:

2.1. Definition of fuzzy set

Assuming X is nonempty set. The set $\tilde{A}$ in X is denoted by ordered pair $\widetilde{A}^{\circ} = \{(x, M(x) : x \in X)\}$. The mapping $M(x) : X \to [0, 1]$ is the membership function and $M(x)$ is the membership value of x in X of the fuzzy set $\widetilde{A}$.

2.2. Definition of triangular fuzzy numbers (TFNs)

Based on the definition of triangular fuzzy numbers (TFNs) from Mondal et al. (2015), the TFNs M is represented by (c_1, c_2, c_3), where $M(x)$ is defined as follows:

$$M(x) = \begin{cases} \frac{x-c_1}{c_2-c_1} \; if \; c_1 \le x \le c_2 \\ 1 \quad if \; x = c_2 \\ \frac{c_3-x}{c_3-c_2} \; if \; c_2 \le x \le c_3 \\ 0 \quad otherwise \end{cases}.$$

2.3. Definition of α cut of a fuzzy number

Based on the definition of α cut of a fuzzy number from Mondal et al. (2015), a fuzzy set $\widetilde{A}$ in X is a mapping $\widetilde{A}: X \to [0, 1]$, where X is the nonempty set. A_α represent the α cut of a fuzzy number $\tilde{A}$ in X. The set $A_\alpha = \{x \in X : A(x) > \alpha\}$ is called α cut of $\widetilde{A}$.

The α cut of a TFN $M = (c_1, c_2, c_3)$ is closed and bounded interval $[M_L(\alpha), M_R(\alpha)]$, where $M_L(\alpha) = c_1 + \alpha(c_2 - c_1)$ and $M_R(\alpha) = c_3 - \alpha(c_3 - c_2)$, where $\alpha \in [0, 1]$.

2.4. Definition of utility function method

Based on the definition of the utility function method from Panja et al. (2017), a utility function can be formed by $w_i h_i(x)$, for i-th objective. The total utility function is prescribed as follows: $U = \sum_{i=1}^{p} w_i h_i(x)$, $w_i > 0$, $i = 1, 2, \ldots\ldots p$, subject to the condition $\sum_{i=1}^{p} w_i = 1$.

where w_i and h_i denote the scalar and the relative value of the objective of utility function, respectively.

3. Model Calibration

Let the total population be $N(t)$. We divide the total population into seven sub populations. They are namely susceptible $(S(t))$, exposed $(E(t))$, quarantined $(Q(t))$, asymptomatic $(A(t))$, symptomatic $(I(t))$, isolation $(M(t))$, and recovered $(R(t))$ population. When the population is symptomatic infectious, they have been transferred to the isolation ward. We have organized this work as SEQAIMR model. For making this model more realistic, we have supposed that $d(> 0)$ is the natural death rate of all seven subpopulation in India. We add another parameter $\Pi(> 0)$ which is the rate per unit time of net influx of susceptible individuals in the environments.

3.1. Crisp model

3.1.1. Dynamics of susceptible population: S(t)

We assume that Π is the rate of recruiting individuals. The parameter d represents natural death rate. Susceptible population converted into quarantine individuals at rate β_1. The susceptible population is sent to safe area for panic. So, we have the differential equation of the susceptible population:

$$\frac{dS}{dt} = \Pi - \lambda SE - \beta_1 S - dS$$

3.1.2. Dynamics of exposed population: E(t)

The parameter λ is the increasing rate of exposed population by the disease transmission between a susceptible population and infected population. The parameter β_2 is the decreasing rate of this population for quarantine. The parameter d represents the natural mortality rate. The exposed population becomes infected at the rate of r_1. The equation of exposed population is controlled in the following way:

$$\frac{dE}{dt} = \lambda SE - r_1 E - \beta_2 E - dE$$

3.1.3. Dynamics of quarantine population: Q(t)

The disease transmission rate is very high during incubation period of the virus. For this reason, the government advises for 14 days of quarantine to control the epidemic. Quarantine population increases at rate β_1 and β_2 from susceptible and exposed population accordingly. This population reduces at rate r_2 and σ_1 due to infected population and recovery rate, respectively. The parameter d represents the natural death rate. Therefore, the quarantine population is given as follows:

$$\frac{dQ}{dt} = \beta_1 S + \beta_2 E - r_2 Q - \sigma_1 Q - dQ$$

3.1.4. Dynamics of asymptomatic population: A(t)

There are no symptoms of COVID-19, but asymptomatic individuals were irradiated to the virus. At a rate γ_1, the exposed individuals converted to asymptomatic. The parameters σ_2 and d are the recovery rate and death rate of the asymptomatic population, respectively. The equation of the asymptomatic population represents in the following way:

$$\frac{dA}{dt} = \gamma_1 E - (\sigma_2 + d)A$$

3.1.5. Dynamics of symptomatic population: I(t)

There are clinical symptoms of COVID-19 of the symptomatic population. The isolation rate of symptomatic individuals is γ_2. The parameter d represents the natural mortality rate and σ_3 is the recovery rate of this population. The equation of the symptomatic population is given below:

$$\frac{dI}{dt} = r_1E + r_2Q - (\sigma_3 + \gamma_2 + d)I$$

3.1.6. Dynamics of isolation population: $\mathbf{M(t)}$

The parameter k is the rate from quarantine community to isolated individuals and γ_2 is the rate from symptomatic groups. The healing rate of isolated individuals is σ_4 and δ is the disease incited death rate and d presents natural mortality rate of this population.

$$\frac{dM}{dt} = kQ + \gamma_2 I - (\delta + \sigma_4 + d)M$$

3.1.7. Dynamics of recovered population: $\mathbf{R(t)}$

The parameters σ_1, σ_2, σ_3, σ_4 represent the rate of heal from quarantine, asymptomatic, symptomatic, and isolated population, respectively.

$$\frac{dR}{dt} = \sigma_1 Q + \sigma_2 A + \sigma_3 I + \sigma_4 M - dR$$

With the help of above consideration, we have got the following dynamical system:

$$\frac{dS}{dt} = \Pi - \lambda SE - \beta_1 S - dS$$

$$\frac{dE}{dt} = \lambda SE - r_1 E - \beta_2 E - dE$$

$$\frac{dQ}{dt} = \beta_1 S + \beta_2 E - r_2 Q - \sigma_1 Q - dQ$$

$$\frac{dA}{dt} = \gamma_1 E - (\sigma_2 + d)A$$

$$\frac{dI}{dt} = r_1 E + r_2 Q - (\sigma_3 + \gamma_2 + d)I$$

$$\frac{dM}{dt} = kQ + \gamma_2 I - (\delta + \sigma_4 + d)M$$

Figure 1
SEQAIMR model diagram

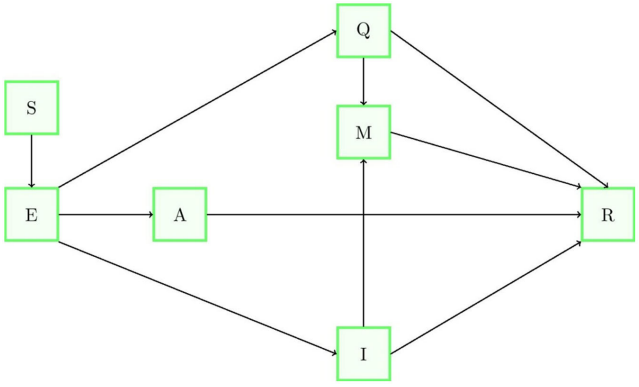

$$\frac{dR}{dt} = \sigma_1 Q + \sigma_2 A + \sigma_3 I + \sigma_4 M - dR. \quad (1)$$

Initially, the state variables are positive. Figure 1 represents the compartment diagram.

3.2. Fuzzy model

In this subsection, using the fuzzy set theory we extend the crisp model (1) with the help of imprecise biological parameters. Then the crisp model (1) reduces the following form:

$$\frac{\widetilde{dS}}{dt} = \widetilde{\Pi} - \widetilde{\lambda} SE - \widetilde{\beta_1} S - \widetilde{d} S$$

$$\frac{\widetilde{dE}}{dt} = \widetilde{\lambda} SE - \widetilde{r_1} E - \widetilde{\beta_2} E - \widetilde{d} E$$

$$\frac{\widetilde{dQ}}{dt} = \widetilde{\beta_1} S + \widetilde{\beta_2} E - \widetilde{r_2} Q - \widetilde{\sigma_1} Q - \widetilde{d} Q$$

$$\frac{\widetilde{dA}}{dt} = \widetilde{\gamma_1} E - \widetilde{\sigma_2} A - \widetilde{d} A$$

$$\frac{\widetilde{dI}}{dt} = \widetilde{r_1} E + \widetilde{r_2} Q - (\widetilde{\gamma_2} + \widetilde{\sigma_3} + \widetilde{d}) I$$

$$\frac{\widetilde{dM}}{dt} = \widetilde{k} Q + \widetilde{\gamma_2} I - (\widetilde{\delta} + \widetilde{\sigma_4} + \widetilde{d}) M$$

$$\frac{\widetilde{dR}}{dt} = \widetilde{\sigma_1} Q + \widetilde{\sigma_2} A + \widetilde{\sigma_3} I + \widetilde{\sigma_4} M - \widetilde{d} R \quad (2)$$

We have to find the solution of the system (2)

$$\left[\frac{dx}{dt}\right]_\alpha = \left[\left(\frac{dx}{dt}\right)_L^\alpha, \left(\frac{dx}{dt}\right)_R^\alpha\right].$$

We get the solution of the system (2) in the following way:

$$\left(\frac{dS}{dt}\right)_L^\alpha = (\Pi_L)^\alpha - (\lambda_R)^\alpha SE - \left(\beta_{1_R}\right)^\alpha S - (d_R)^\alpha S$$

$$\left(\frac{dS}{dt}\right)_R^\alpha = (\Pi_R)^\alpha - (\lambda_L)^\alpha SE - \left(\beta_{1_L}\right)^\alpha S - (d_L)^\alpha S$$

$$\left(\frac{dE}{dt}\right)_L^\alpha = (\lambda_L)^\alpha SE - \left(r_{1_R}\right)^\alpha E - \left(\beta_{2_R}\right)^\alpha E - (d_R)^\alpha E$$

$$\left(\frac{dE}{dt}\right)_R^\alpha = (\lambda_R)^\alpha SE - \left(r_{1_L}\right)^\alpha E - \left(\beta_{2_L}\right)^\alpha E - (d_L)^\alpha E$$

$$\left(\frac{dQ}{dt}\right)_L^\alpha = \left(\beta_{1_L}\right)^\alpha S + \left(\beta_{2_L}\right)^\alpha E - \left(r_{2_R}\right)^\alpha Q - \left(\sigma_{1_R}\right)^\alpha Q - (k_R)^\alpha Q - (d_R)^\alpha Q$$

$$\left(\frac{dQ}{dt}\right)_R^\alpha = \left(\beta_{1_R}\right)^\alpha S + \left(\beta_{2_R}\right)^\alpha E - \left(r_{2_L}\right)^\alpha Q - \left(\sigma_{1_L}\right)^\alpha Q - (k_L)^\alpha Q - (d_L)^\alpha Q$$

$$\left(\frac{dA}{dt}\right)_L^\alpha = \left(\gamma_{1_L}\right)^\alpha E - \left(\sigma_{2_R}\right)^\alpha A - (d_R)^\alpha A$$

$$\left(\frac{dA}{dt}\right)_R^\alpha = \left(\gamma_{1_R}\right)^\alpha E - \left(\sigma_{2_L}\right)^\alpha A - (d_L)^\alpha A$$

$$\left(\frac{dI}{dt}\right)_L^{\alpha}=(r_{1_L})^{\alpha}E+(r_{2_L})^{\alpha}Q-\left[(\gamma_{2_R})^{\alpha}+(\sigma_{3_R})^{\alpha}+(d_R)^{\alpha}\right]I$$

$$\left(\frac{dI}{dt}\right)_R^{\alpha}=(r_{1_R})^{\alpha}E+(r_{2_R})^{\alpha}Q-\left[(\gamma_{2_L})^{\alpha}+(\sigma_{3_L})^{\alpha}+(d_L)^{\alpha}\right]I$$

$$\left(\frac{dM}{dt}\right)_L^{\alpha}=(k_L)^{\alpha}Q+(\gamma_{2_L})^{\alpha}I-\left[(\delta_R)^{\alpha}+(\sigma_{4_R})^{\alpha}+(d_R)^{\alpha}\right]M$$

$$\left(\frac{dM}{dt}\right)_R^{\alpha}=(k_R)^{\alpha}Q+(\gamma_{2_R})^{\alpha}I-\left[(\delta_L)^{\alpha}+(\sigma_{4_L})^{\alpha}+(d_L)^{\alpha}\right]M$$

$$\left(\frac{dR}{dt}\right)_L^{\alpha}=(\sigma_{1_L})^{\alpha}Q+(\sigma_{2_L})^{\alpha}A+(\sigma_{3_L})^{\alpha}I+(\sigma_{4_L})^{\alpha}M-(d_R)^{\alpha}R$$

$$\left(\frac{dR}{dt}\right)_R^{\alpha}=(\sigma_{1_R})^{\alpha}Q+(\sigma_{2_R})^{\alpha}A+(\sigma_{3_R})^{\alpha}I+(\sigma_{4_R})^{\alpha}M-(d_L)^{\alpha}R. \tag{3}$$

3.3. Defuzzified model

Using UFM, we have defuzzified the fuzzy model. The fuzzy model is reduced in the following forms:

$$\frac{dS}{dt}=w_1\left(\frac{ds}{dt}\right)_L^{\alpha}+w_2\left(\frac{ds}{dt}\right)_R^{\alpha}$$

$$\frac{dE}{dt}=w_1\left(\frac{dE}{dt}\right)_L^{\alpha}+w_2\left(\frac{dE}{dt}\right)_R^{\alpha}$$

$$\frac{dQ}{dt}=w_1\left(\frac{dQ}{dt}\right)_L^{\alpha}+w_2\left(\frac{dQ}{dt}\right)_R^{\alpha}$$

$$\frac{dA}{dt}=w_1\left(\frac{dA}{dt}\right)_L^{\alpha}+w_2\left(\frac{dA}{dt}\right)_R^{\alpha}$$

$$\frac{dI}{dt}=w_1\left(\frac{dI}{dt}\right)_L^{\alpha}+w_2\left(\frac{dI}{dt}\right)_R^{\alpha}$$

$$\frac{dM}{dt}=w_1\left(\frac{dM}{dt}\right)_L^{\alpha}+w_2\left(\frac{dM}{dt}\right)_R^{\alpha}$$

$$\frac{dR}{dt}=w_1\left(\frac{dR}{dt}\right)_L^{\alpha}+w_2\left(\frac{dR}{dt}\right)_R^{\alpha} \tag{4}$$

Here, w_1 and w_2 are two weight functions. They satisfy the conditions $w_1+w_2=1$ and $w_1\geq 0$ and $w_2\geq 0$.

Equation (4) can be written as follows:

$$\frac{dS}{dt}=b_{11}-b_{12}SE-b_{13}S$$

$$\frac{dE}{dt}=b_{21}SE-b_{22}E$$

$$\frac{dQ}{dt}=b_{31}S+b_{32}E-b_{33}Q$$

$$\frac{dA}{dt}=b_{41}E-b_{42}A$$

$$\frac{dI}{dt}=b_{51}E+b_{52}Q-b_{53}I$$

$$\frac{dM}{dt}=b_{61}Q+b_{62}I-b_{63}M$$

$$\frac{dR}{dt}=b_{71}Q+b_{72}A+b_{73}I+b_{74}M-b_{75}R \tag{5}$$

where, $b_{11}=w_1(\Pi_L)^{\alpha}+w_2(\Pi_R)^{\alpha}; b_{12}=w_1(\lambda_R)^{\alpha}+w_2(\lambda_L)^{\alpha}; b_{13}=w_1\left[(\beta_{1_R})^{\alpha}+(d_R)^{\alpha}\right]+w_2\left[(\beta_{1_L})^{\alpha}+(d_L)^{\alpha}\right]; \; b_{21}=w_1(\lambda_L)^{\alpha}+w_2(\lambda_R)^{\alpha}; \; b_{22}=w_1[(r_{1_R})^{\alpha}+(\beta_{2_R})^{\alpha}+(d_R)^{\alpha}]+w_2\left[(r_{1_L})^{\alpha}+(\beta_{2_L})^{\alpha}+(d_L)^{\alpha}\right]; \; b_{31}=w_1(\beta_{1_L})^{\alpha}+w_2(\beta_{1_R})^{\alpha}; b_{32}=w_1(\beta_{2_L})^{\alpha}+w_2(\beta_{2_R})^{\alpha};$

$b_{33}=w_1\left[(r_{2_R})^{\alpha}+(\sigma_{1_R})^{\alpha}+(k_R)^{\alpha}+(d_R)^{\alpha}\right]+w_2[(r_{2_L})^{\alpha}+(\sigma_{1_L})^{\alpha}+(k_L)^{\alpha}+(d_L)^{\alpha}]; \quad b_{41}=w_1(\gamma_{1_L})^{\alpha}+w_2(\gamma_{1_R})^{\alpha}; \; b_{42}=w_1\left[(\gamma_{1_R})^{\alpha}+(d_R)^{\alpha}\right]+w_2[(\gamma_{1_L})^{\alpha}+(d_L)^{\alpha}]; \; b_{51}=w_1(r_{1_L})^{\alpha}+w_2\left(r_{1_R}\right)^{\alpha}; \; b_{52}=w_1(r_{2_L})^{\alpha}+w_2(r_{2_R})^{\alpha}; \quad b_{53}=w_1\left[(\gamma_{2_R})^{\alpha}+(\sigma_{3_R})^{\alpha}+(d_R)^{\alpha}\right]+w_2\left[\left(\gamma_{2_L}\right)^{\alpha}+(\sigma_{3_L})^{\alpha}+(d_L)^{\alpha}\right],$
$b_{61}=w_1(k_L)^{\alpha}+w_2(k_R)^{\alpha}; \; b_{62}=w_1(\gamma_{2_L})^{\alpha}+w_2(\gamma_{2_R})^{\alpha}; \; b_{63}=w_1[(\delta_R)^{\alpha}+(\sigma_{4_R})^{\alpha}+(d_R)^{\alpha}]+w_2\left[(\delta_L)^{\alpha}+(\sigma_{4_L})^{\alpha}+(d_L)^{\alpha}\right]; \; b_{71}=w_1(\sigma_{1_L})^{\alpha}+w_2(\sigma_{1_R})^{\alpha}; \; b_{72}=w_1(\sigma_{2_L})^{\alpha}+w_2(\sigma_{2_R})^{\alpha}; \; b_{73}=w_1(\sigma_{3_L})^{\alpha}+w_2(\sigma_{3_R})^{\alpha}; \; b_{74}=w_1(\sigma_{4_L})^{\alpha}+w_2(\sigma_{4_R})^{\alpha}; b_{75}=w_1(d_R)^{\alpha}+w_2(d_L)^{\alpha}.$

4. Theoretical Study of the Model

In this section, we have discussed the nature of the system.

4.1. Boundedness of the system

Theorem 1: *The system (5) is entirely bounded if the condition* $\psi=min\{(b_{13}-b_{31}),\ (b_{22}-b_{32}-b_{41}-b_{51}),\ (b_{33}-b_{52}-b_{61}),\ (b_{53}-b_{62}),\ b_{42},b_{63}\}$, *and* $b_{21}>b_{12}$ *are satisfied.*

Proof: Let us consider auxiliary function

$$F=S+E+Q+A+I+M.$$

Differentiating with respect to t both sides, we derive

$$\frac{dF}{dt}=\frac{dS}{dt}+\frac{dE}{dt}+\frac{dQ}{dt}+\frac{dA}{dt}+\frac{dI}{dt}+\frac{dM}{dt}$$

$\frac{dF}{dt}+\psi F=b_{11}+(b_{21}-b_{12})SE+(b_{31}-b_{13}+\psi)S+(b_{32}+b_{41}+b_{51}-b_{22}+\psi)E+(b_{52}+b_{61}-b_{33}+\psi)Q+(-b_{42}+\psi)A+(b_{62}-b_{53}+\psi)I+(\psi-b_{63})M=b_{11}+(b_{21}-b_{12})SE+\{\psi-b_{13}+b_{31}\}S+\{\psi-(b_{22}-b_{32}-b_{41}-b_{51})\}E+\{\psi-(b_{33}-b_{52}-b_{61})\}Q+(\psi-b_{42})A+\{\psi-(b_{53}-b_{62})I+(\psi-b_{63})M\}.$

Choosing $\psi=min\{(b_{13}-b_{31}),\ (b_{22}-b_{32}-b_{41}-b_{51}),\ (b_{33}-b_{52}-b_{61}),\ (b_{53}-b_{62}),\ b_{42},b_{63}\}$ and $b_{21}>b_{12}$,

We get $\frac{dF}{dt}+\psi F\leq b_{11}$.

The solution of the equation is $F\leq\frac{b_{11}}{\psi}+c_1e^{-\psi t}$.

Therefore, $F\leq\frac{b_{11}}{\psi}$, as $t\to\infty$.

Consequently, we can conclude $S(t) \leq \frac{b_{11}}{\psi}$, $E(t) \leq \frac{b_{11}}{\psi}$, $Q(t) \leq \frac{b_{11}}{\psi}$, $A(t) \leq \frac{b_{11}}{\psi}$, $I(t) \leq \frac{b_{11}}{\psi}$, $M(t) \leq \frac{b_{11}}{\psi}$.

We put the value of $Q(t)$, $A(t)$, $I(t)$, $M(t)$ in the system (5)

$$\frac{dR}{dt} \leq \frac{b_{11}}{\psi}(b_{71} + b_{72} + b_{73} + b_{74}) - b_{75}R$$

$$\frac{dR}{dt} + b_{75}R \leq \frac{b_{11}}{\psi}(b_{71} + b_{72} + b_{73} + b_{74})$$

The solution of the above inequality is given by

$$R(t) \leq \frac{b_{11}}{\psi}(b_{71} + b_{72} + b_{73} + b_{74}) + c_2 e^{-b_{75}t}.$$

When t tends to ∞, the solution becomes $R(t) \leq \frac{b_{11}}{\psi}(b_{71} + b_{72} + b_{73} + b_{74})$.

Hence, we have concluded that the solution of the system (5) becomes bounded under the conditions $\psi = min\{(b_{13} - b_{31}), (b_{22} - b_{32} - b_{41} - b_{51}), (b_{33} - b_{52} - b_{61}), (b_{53} - b_{62}), b_{42}, b_{63}\}$ and $b_{21} > b_{12}$.

4.2. Equilibria

The following equation gives the equilibrium points.

$$b_{11} - b_{12}SE - b_{13}S = 0$$

$$b_{21}SE - b_{22}E = 0$$

$$b_{31}S + b_{32}E - b_{33}Q = 0$$

$$b_{41}E - b_{42}A = 0$$

$$b_{51}E + b_{52}Q - b_{53}I = 0$$

$$b_{61}Q + b_{62}I - b_{63}M = 0$$

$$b_{71}Q + b_{72}A + b_{73}I + b_{74}M - b_{75}R = 0$$

(a) Infection-free steady state is denoted by $E_1{}^0\left(S^0, E^0, Q^0, A^0, I^0, M^0, R^0\right) = \left(\frac{b_{11}}{b_{13}}, 0, 0, 0, 0, 0, 0\right)$.

(b) The endemic equilibrium is $E_1{}^* = (S^*, E^*, Q^*, A^*, I^*, M^*, R^*)$

where, $S^* = \frac{b_{22}}{b_{21}}$, $E^* = \frac{b_{11}b_{21} - b_{13}b_{22}}{b_{12}b_{22}}$ $\frac{Q^* = b_{31}b_{22}b_{12}b_{22} + b_{32}b_{21}(b_{11}b_{21} - b_{13}b_{22})}{b_{12}b_{21}b_{22}b_{33}}$, $A^* = \frac{b_{41}(b_{11}b_{21} - b_{13}b_{22})}{b_{42}b_{12}b_{22}}$, $I^* = \frac{b_{51}E^* + b_{52}Q^*}{b_{53}}$, $M^* = \frac{b_{61}Q^* + b_{62}I^*}{b_{63}}$, $R^* = \frac{b_{71}Q^* + b_{72}A^* + b_{73}I^* + b_{74}M^*}{b_{75}}$.

4.3. Basic reproduction number (R_0)

With the help of the next generation matrix method (van den Driessche & Watmough, 2002), we calculate the basic reproduction number. From the system (5), we have

$$\frac{dy}{dt} = \varphi(v) - \chi(v)$$

where, $v = \begin{pmatrix} E \\ Q \\ A \\ I \\ M \\ R \\ S \end{pmatrix}$; $\varphi(v) = \begin{pmatrix} b_{21}SE \\ 0 \\ 0 \\ 0 \\ 0 \\ 0 \\ 0 \end{pmatrix}$

and $\chi(v) = \begin{pmatrix} b_{22}E \\ -b_{31}S - b_{32}E + b_{33}Q \\ -b_{41}E + b_{42}A \\ -b_{51}E - b_{52}Q + b_{53}I \\ -b_{61}Q - b_{62}I + b_{63}M \\ -b_{71}Q - b_{72}A - b_{73}I - b_{74}M + b_{75}R \\ -b_{11} + b_{12}SE + b_{13}S \end{pmatrix}$.

Now, we analyze the Jacobian matrix of ϕ and χ at $E_1{}^0$

$$J\left(\varphi|_{E_1{}^0}\right) = \begin{pmatrix} F & 0 \\ 0 & 0 \end{pmatrix} \text{ where, } F = \begin{pmatrix} \frac{b_{11}b_{21}}{b_{13}} & 0 \\ 0 & 0 \end{pmatrix}$$

$$J\left(\chi|_{E_1{}^0}\right) = \begin{pmatrix} V_2 & K_1 \\ K_2 & K_3 \end{pmatrix} \quad \text{where,} \quad V_2 = \begin{pmatrix} b_{22} & 0 \\ -b_{32} & b_{33} \end{pmatrix};$$

$K_1 = \begin{pmatrix} 0 & 0 & 0 & 0 & 0 \\ 0 & 0 & 0 & 0 & -b_{31} \end{pmatrix}$;

$K_2 = \begin{pmatrix} -b_{41} & 0 & b_{42} \\ -b_{51} & -b_{52} & 0 \\ 0 & -b_{61} & 0 \\ 0 & -b_{71} & -b_{72} \\ \frac{b_{11}b_{12}}{b_{13}} & 0 & 0 \end{pmatrix}$; $K_3 = \begin{pmatrix} 0 & 0 & 0 & 0 \\ b_{53} & 0 & 0 & 0 \\ -b_{62} & b_{63} & 0 & 0 \\ -b_{73} & -b_{74} & b_{75} & 0 \\ 0 & 0 & 0 & b_{13} \end{pmatrix}$

Now, we derive $R_0 = FV_2{}^{-1} = \frac{b_{11}b_{21}}{b_{13}b_{22}}$.

Therefore,

$R_0 = \frac{[w_1(\Pi_L)^\alpha + w_2(\Pi_R)^\alpha][w_1(\lambda_L)^\alpha + w_2(\lambda_R)^\alpha]}{\{w_1[(\beta_{1R})^\alpha + (d_R)^\alpha] + w_2[(\beta_{1_L})^\alpha + (d_L)^\alpha]\}\{w_1[(r_{1R})^\alpha + (\beta_{2R})^\alpha + (d_R)^\alpha] + w_2[(r_{1_L})^\alpha + (\beta_2)^\alpha + (d_R)^\alpha]\}}$.

4.4. Stability analysis

In this section, two feasible steady states of SEQAIMR model are investigated. The equilibrium points in steady states are stable or unstable the conditions represented in the following theorems.

Theorem 2: *Under the condition $R_0 < 1$ and $R_0 > 1$, the infection-free equilibrium $E_1{}^0$ of the system (5) is locally asymptotically stable and unstable, respectively.*

Proof: At the infection-free equilibrium point ($E_1{}^0$), we get

$$J_{E_1{}^0} = \begin{pmatrix} -b_{13} & -\frac{b_{12}b_{11}}{b_{13}} & 0 & 0 & 0 & 0 & 0 \\ 0 & \frac{b_{21}b_{11} - b_{22}b_{13}}{b_{13}} & 0 & 0 & 0 & 0 & 0 \\ b_{31} & b_{32} & -b_{33} & 0 & 0 & 0 & 0 \\ 0 & b_{41} & 0 & -b_{42} & 0 & 0 & 0 \\ 0 & b_{51} & b_{52} & 0 & -b_{53} & 0 & 0 \\ 0 & 0 & b_{61} & 0 & b_{62} & -b_{63} & 0 \\ 0 & 0 & b_{71} & b_{72} & b_{73} & b_{74} & -b_{75} \end{pmatrix}$$

The five negative eigenvalues of the matrix are $-b_{33}$, $-b_{42}$, $-b_{53}$, $-b_{63}$, and $-b_{75}$. The quadratic equation $x^2 + g_1 x + g_2 = 0$ represents other eigenvalues, where $g_1 = b_{13} + \frac{b_{11}b_{21} - b_{13}b_{22}}{b_{13}}$, $g_2 = b_{13}b_{22} - b_{11}b_{21} = b_{13}b_{22}(1 - R_0)$.

Here, all the involved model parameter values are negative: $-b_{33} < 0$, $-b_{42} < 0$, $-b_{53} < 0$, $-b_{63} < 0$, $-b_{75} < 0$. If, $g_1 > 0$, $g_2 > 0$, and $g_1^2 - 4g_2 < 0$, the roots of quadratic equation are negative. Therefore, we have $(1 - R_0) > 0$ or $R_0 < 1$. If $R_0 < 1$, the infection-free equilibrium ${E_1}^0$ is locally asymptotically stable and unstable if $R_0 > 1$.

Theorem 3: Under the condition $R_0 < 1$, the infection-free equilibrium ${E_1}^0$ of the system (5) is globally asymptotically stable.

Proof: We rewrite the system (5) as

$$\frac{dU}{dt} = L_1(U, V)$$

$$\frac{dV}{dt} = L_2(U, V), \quad L_2(U, 0) = 0$$

where $U = (S, R) \in R^2$, which represents the number of uninfected populations, $V = (E, Q, A, I, M) \in R^5$, which represent the number of infected populations. We represent infection-free equilibrium point ${E_1}^0 = \left(\frac{b_{11}}{b_{13}}, 0, 0, 0, 0, 0, 0\right)$ of the system (5). The global stability of the infection-free equilibrium is maintained by two conditions (i) and (ii).

(i) If $\frac{dU}{dt} = L_1(U, 0)$, U^0 becomes the globally asymptotically stable
(ii) If $L_2(U, V) \geq 0$ for $(U, V) \in \Omega$, then $L_2(U, V) = BV - {L_2}^*(U, V)$.

where $B = D_z L_1(U^0, 0)$ has non-negative off-diagonal elements.

With the help of Castillo-Chavez and Song (2004), we define the system (5), $L_1(U, 0) = \begin{pmatrix} b_{11} - b_{13}S \\ 0 \end{pmatrix}$

$$B = \begin{pmatrix} b_{11} - b_{22} & 0 & 0 & 0 & 0 \\ b_{32} & -b_{33} & 0 & 0 & 0 \\ b_{41} & 0 & -b_{42} & 0 & 0 \\ b_{51} & b_{52} & 0 & -b_{53} & 0 \\ 0 & b_{61} & 0 & b_{62} & -b_{63} \end{pmatrix}$$

$$BV - {L_2}^*(U, V) = \begin{pmatrix} b_{11} - b_{22} & 0 & 0 & 0 & 0 \\ b_{32} & -b_{33} & 0 & 0 & 0 \\ b_{41} & 0 & -b_{42} & 0 & 0 \\ b_{51} & b_{52} & 0 & -b_{53} & 0 \\ 0 & b_{61} & 0 & b_{62} & -b_{63} \end{pmatrix} \begin{pmatrix} E \\ Q \\ A \\ I \\ M \end{pmatrix} - \begin{pmatrix} b_{12}SE \\ b_{31}S \\ 0 \\ 0 \\ 0 \end{pmatrix}.$$

${L_2}^*(U, V) \geq 0$ when the state variables are in the region Ω. B illustrates the Metzler matrix. Therefore, both the conditions (i) and (ii) are satisfied. Hence, the proof is completed.

Theorem 4: *If all of* $A_i(A_1, A_2, A_3, A_4, A_5, A_6)$ *and* $\Gamma_2, \Gamma_3, \Gamma_4, \Gamma_5$ *are positive, then the system (5) becomes locally asymptotically stable at* ${E_1}^*$.

Proof: At ${E_1}^*$, the equation becomes

$$-(x + b_{75})(x^6 + A_1x^5 + A_2x^4 + A_3x^2 + A_4x + A_5) = 0$$

where $A_1 = b_{13} + b_{22} + b_{33} + b_{42} + b_{53} + b_{63} - b_{21}S^* + b_{12}E^* + b_{12}b_{21}S^*E^*$

$A_2 = (b_{22} - b_{21}S^*)(b_{13} + b_{12}E^*) + (b_{13} + b_{12}E^* + b_{22} - b_{21}S^*)(b_{33} + b_{42} + b_{53} + b_{63}) + b_{33}b_{42} + b_{53}b_{63} + (b_{33} + b_{42})(b_{53} + b_{63}) + b_{12}b_{21}S^*E^*(b_{33} + b_{42} + b_{53} + b_{63} + b_{13} + b_{21}E^*)$

$A_3 = (b_{13} + b_{12}E^* + b_{22} - b_{21}S^*)[(b_{33} + b_{42})(b_{53} + b_{63}) + b_{33}b_{42} + b_{53}b_{63}] + (b_{33} + b_{42})b_{53}b_{63} + b_{33}b_{42}(b_{53} + b_{63}) + b_{12}b_{21}S^*E^*[(b_{13} + b_{21}E^*)(b_{33} + b_{42} + b_{53} + b_{63}) + (b_{33}b_{42} + b_{53}b_{63} + (b_{33} + b_{42})(b_{53} + b_{63})$

$A_4 = b_{33}b_{42}b_{53}b_{63} + (b_{13} + b_{12}E^* + b_{22} - b_{21}S^*)\{(b_{33} + b_{42})b_{53}b_{63} + b_{33}b_{42}(b_{53} + b_{63})\} + b_{33}b_{42}b_{53}b_{63} + b_{12}b_{21}S^*E^*\{(b_{13} + b_{21}E^*)(b_{33}b_{42}(b_{33} + b_{42})(b_{53} + b_{63}) + b_{53}b_{63}) + [(b_{33} + b_{42}) + b_{53}b_{63} + b_{33}b_{42}(b_{53} + b_{63})]\}$

$A_5 = (b_{13} + b_{12}E^* + b_{22} - b_{21}S^* + 1)b_{33}b_{42}b_{53}b_{63} + (b_{13} + b_{12}E^*)(b_{22} - b_{21}S^*)(b_{33} + b_{42})b_{53}b_{63} + (b_{53} + b_{63})b_{33}b_{42} + b_{12}b_{21}S^*E^*\{(b_{13} + b_{12}E^*)[(b_{33} + b_{42})b_{53}b_{63} + (b_{33}b_{42})(b_{53} + b_{63})]$

$A_6 = b_{33}b_{42}b_{53}b_{63}\{(b_{13} + b_{12}E^*)(b_{22} - b_{21}S^*)\} + b_{12}b_{21}S^*E^*(b_{13} + b_{12}E^*)$.

We define the following terms:

$\Gamma_1 = A_1$, $\Gamma_2 = A_1A_2 - A_3$, $\Gamma_3 = A_1A_2A_3 - {A_1}^2A_4 - {A_3}^2 + A_1A_5$

$\Gamma_4 = A_6{A_1}^2A_2 - {A_1}^2{A_4}^2 - A_1{A_2}^2A_5 + A_1A_2A_3A_4 - A_6A_1A_3 + 2A_1A_4A_5 + A_2A_3A_5 - {A_3}^2A_4 - {A_5}^2$

$\Gamma_5 = -{A_1}^3{A_6}^2 + 2{A_1}^2A_2A_5A_6 + {A_1}^2A_3A_4A_6 - {A_1}^2{A_4}^2A_5 - A_1{A_2}^2{A_5}^2 - A_1A_2{A_3}^2A_6 + A_1A_2A_3A_4A_5 - 3A_1A_3A_5A_6 + 2A_1A_4{A_5}^2 + A_2A_3{A_5}^2 + {A_3}^3A_6 - {A_3}^2A_4A_5 - {A_5}^3$.

Applying the Routh Hurwitz criteria, the system (5) becomes locally asymptotically stable at ${E_1}^*$ under the conditions $A_i(i = 1, 2, 3, 4, 5, 6) > 0$ and $\Gamma_i(i = 1, 2, 3, 4, 5, 6) > 0$.

Theorem 5: *Under the condition* $\psi_2 = b_{21}u_1 - b_{22} + b_{33} - b_{32} + \min[b_{21}u_1 + b_{13} + b_{22}] + min[b_{13} + u_1(b_{21} - b_{12}), b_{22}] > 0$, *the endemic equilibrium* ${E_1}^*$ *of the system* (5) *will be globally asymptotically stable.*

Proof: From (5), we choose a subsystem

$$\frac{dS}{dt} = b_{11} - b_{12}SE - b_{13}S$$

$$\frac{dE}{dt} = b_{21}SE - b_{22}E$$

$$\frac{dQ}{dt} = b_{31}S + b_{32}E - b_{33}Q \tag{6}$$

The system (6) is written as follows

$$M = \begin{pmatrix} -b_{12}E - b_{13} & -b_{12}S & 0 \\ b_{21}E & -b_{22} & 0 \\ b_{31} & b_{32} & -b_{33} \end{pmatrix}$$

With the help of Buonomo et al. (2008), we have the second additive compound matrix as follows

$$M^{[2]} = \begin{pmatrix} -b_{12}E - b_{13} - b_{22} & 0 & 0 \\ b_{32} & -b_{12}E - b_{13} - b_{33} & -b_{12}S \\ -b_{31} & b_{21}E & -b_{22} - b_{33} \end{pmatrix}$$

Let us assume the function

$$D\,(S,\ E,\ Q)\ =\ \text{diag}\left\{\frac{S}{E}, \frac{S}{E}, \frac{S}{E}\right\}$$

$$D_f = \frac{\partial D}{\partial x} = \text{diag}\left(\frac{\dot{S}}{E} - \frac{S\dot{E}}{E^2}, \frac{\dot{S}}{E} - \frac{S\dot{E}}{E^2}, \frac{\dot{S}}{E} - \frac{S\dot{E}}{E^2}\right).$$

It gives us $D_f D^{-1} = \text{diag}\ (\frac{\dot{S}}{E} - \frac{\dot{E}}{E}, \frac{\dot{S}}{S} - \frac{\dot{E}}{E}, \frac{\dot{S}}{S} - \frac{\dot{E}}{E})$ and $DJ^{[2]}D\ =\ J^{[2]}$.

Then, we get $L\ =\ D_f D^{-1} + DJ^{[2]}D\ =\ \begin{pmatrix} L_{11} & L_{12} \\ L_{21} & L_{22} \end{pmatrix}$

where, $L_{11} = \frac{\dot{S}}{S} - \frac{\dot{E}}{E} - (b_{12}E + b_{13} + b_{22})$, $L_{12} = (0,\ 0)$, $L_{21} = (b_{32} - b_{31})^T$

$$L_{22} = \begin{pmatrix} \frac{\dot{S}}{S} - \frac{\dot{E}}{E} - (b_{12}E + b_{13} + b_{33}) & -b_{12}S \\ b_{21}E & \frac{\dot{S}}{S} - \frac{\dot{E}}{E} - (b_{22} + b_{33}) \end{pmatrix}$$

We consider the norm in R^3 as $|(\ x,\ y, z)| = \max\ \{\ |x|,\ |y + z|\}$ where $(x,\ y,\ z)$ any vector in R^3 and represented by R. Therefore,

$$R(L) \leq\ \sup\{\mathrm{r}_1,\ \mathrm{r}_2\} = \sup\{R(L_{11}) + |L_{12}|,\ R(L_{22}) + |L_{21}|\ \} \quad (7)$$

where, $|\mathrm{L}_{12}|$ and $|\mathrm{L}_{21}|$ represent matrix norms according to R norms. Thus

$h_1 =\ R(L_{11}) + |L_{12}|$

where, $R(L_{11}) = \frac{\dot{\mathrm{S}}}{\mathrm{S}} - \frac{\dot{\mathrm{E}}}{\mathrm{E}} - (\mathrm{b}_{12}\mathrm{E} + \mathrm{b}_{13} + \mathrm{b}_{22})$ and $|\mathrm{L}_{12}| = 0$

We have $r_1 = \frac{\dot{\mathrm{S}}}{\mathrm{S}} - \frac{\dot{\mathrm{E}}}{\mathrm{E}} - (\mathrm{b}_{12}\mathrm{E} + \mathrm{b}_{13} + \mathrm{b}_{22})$

and $r_2 = \&R(L_{22}) + |L_{21}|$

$$= \frac{\dot{S}}{S} - \frac{\dot{E}}{E} - b_{33} + b_{32} - min\{b_{13} + E(b_{21} - b_{12}),\ b_{22}\ \} \quad (8)$$

We have $\dot{E} = b_{21}SE - b_{22}E$

$$\frac{\dot{E}}{E} = b_{21}S - b_{22}.$$

Substituting the value of $\frac{\dot{E}}{E}$ in (8) and there exist $t_1 > 0$ such that

$u_1 = \inf\{S(t),\ E(t),\ Q(t)\}$

We get $r_1 = \frac{\dot{\mathrm{S}}}{\mathrm{S}} - b_{21}u_1 + b_{22} - (b_{12}u_1 + b_{13} + b_{22}\ )$

$$r_2 = \frac{\dot{S}}{S} - b_{21}u_1 + b_{22} - b_{33} + b_{32} - min\{b_{13} + u_1(b_{21} - b_{12}),\quad b_{22}\}$$

$R(L) \leq sup\{r_1, r_2\ \}$

$$\leq \frac{\dot{S}}{S} - b_{21}u_1 + b_{22} - b_{33} + b_{32} - \min\{(b_{12}u_1 + b_{13} + b_{22})\} - min\{b_{13} + u_1(b_{21} - b_{12}),\quad b_{22}\}$$

$$\text{i.e. } R(\mathrm{L}\ ) \leq \frac{\dot{\mathrm{S}}}{\mathrm{S}} - \psi_2 \quad (9)$$

where, $\psi_2 = b_{21}u_1 - b_{22} + b_{33} - b_{32} + \min\{(b_{12}u_1 + \mathrm{b}_{13} + \mathrm{b}_{22})\} + \min\{\mathrm{b}_{13} + u_1(b_{21} - b_{12}),\quad b_{22}\ \}$

Integrating both sides, we have

$$\int_0^t R(L\ )ds\ \leq log\frac{S(t)}{S(0)} - \psi_2 t$$

$$\frac{1}{t}\int_0^t R(L\ )ds\ \leq \frac{1}{t}\ log\frac{S(t)}{S(0)} - \psi_2$$

$\lim_{t\to\infty} sup\ sup\ \frac{1}{t}\int_0^t R(L\ )ds\ < -\psi_2 < 0$ if $\psi_2 > 0$.

Hence, we can say that (S^*, E^*, Q^*) will be globally asymptotically stable if $\psi_2 > 0$. Now the remaining part of the system (5) is as follows:

$$\frac{dA}{dt} = b_{41}E - b_{42}A$$

$$\frac{dI}{dt} = b_{51}E + b_{52}Q - b_{53}I$$

$$\frac{dM}{dt} = b_{61}Q + b_{62}I - b_{63}M$$

$$\frac{dR}{dt} = b_{71}Q + b_{72}A + b_{73}I + b_{74}M - b_{75}R \quad (10)$$

Its limit system becomes

$$\frac{dA}{dt} = b_{41}E^* - b_{42}A^* \quad \text{(i)}$$

$$\frac{dI}{dt} = b_{51}E^* + b_{52}Q^* - b_{53}I^* \quad \text{(ii)}$$

$$\frac{dM}{dt} = b_{61}Q^* + b_{62}I^* - b_{63}M^* \quad \text{(iii)}$$

$$\frac{dR}{dt} = b_{71}Q^* + b_{72}A^* + b_{73}I^* + b_{74}M^* - b_{75}R^* \quad \text{(iv)}$$

From (i), the solution is

$$A(t)\ =\ A(0)\ e^{-b_{42}t} + \frac{b_{41}}{b_{42}}E^* - b_{41}e^{-b_{42}t}E^*$$

This implies $A(t)\ \to\ \frac{b_{41}}{b_{42}}E^* =\ A^*$ as $t \to \infty$.

The equation (ii) gives us $I(t)\ =\ I(0)\ e^{-b_{53}t} + \frac{b_{51}E^* + b_{52}Q^*}{b_{53}} - (b_{51}E^* + b_{52}Q^*\ )e^{-b_{53}t}$

It indicates $I(t) \to \frac{b_{51}E^* + b_{52}Q^*}{b_{53}} = I^*$ as $t \to \infty$.

In similar way from (iii) and (iv) it follows, $M(t) \to M^*$ and $R(t) \to R^*$ when t tends to ∞.

Hence, the system (6) will be globally asymptotically stable at $E_1{}^*$.

5. Optimal Control Analysis

We discuss that how proper control policy diminishes the disease from the population. So, the precautionary measures such as maintaining social distance and use of face mask in mass gathering area are important factors to diminish the spread of disease. We take the incurred cost that needs to minimize by applying control intervention. Using the maximum principle from Pontryagin et al. (1962), the objective functional can be represented as

$$L_1 = min_{\nu_1,\nu_2} \int_0^{T_1} (k_1 I + k_2 {\nu_1}^2 + k_3 {\nu_2}^2) dt$$

with subject to the condition

$$\frac{dS}{dt} = \Pi - (1-\nu_1)\lambda SE - \beta_1 S - dS - \nu_2 S$$

$$\frac{dE}{dt} = (1-\nu_1)\lambda SE - r_1 E - \beta_2 E - dE$$

$$\frac{dQ}{dt} = \beta_1 S + \beta_2 E - r_2 Q - \sigma_1 Q - dQ$$

$$\frac{dA}{dt} = \gamma_1 E - (\sigma_2 + d)A$$

$$\frac{dI}{dt} = r_1 E + r_2 Q - (\sigma_3 + \gamma_2 + d)I$$

$$\frac{dM}{dt} = kQ + \gamma_2 I - (\delta + \sigma_4 + d)M$$

$$\frac{dR}{dt} = \nu_2 S + \sigma_1 Q + \sigma_2 A + \sigma_3 I + \sigma_4 M - dR \qquad (11)$$

with $S(0) > 0,\ E(0) > 0,\ Q(0) > 0,\ A(0) > 0,\ I(0) > 0, M(0) > 0,\ R(0) > 0$. Let, the constant k_1 represents the per capita loss due to the presence of infected population at any instants. The control parameter ν_1 is considered as the precautionary measure (like maintaining social distance, use of face mask in mass gathering) and ν_2 as the protective measure (like maintaining suitable hygiene, staying in isolation) for the susceptible population. k_2 and k_3 are the weighted functions of ν_1 and ν_2 respectively and k_1, k_2, k_3 are positive constants in time interval $[0,\ T_1]$. The area of the control intervention $\nu_1(t),\ \nu_2(t)$ is given as follows:

$$\psi = \{(\nu_1(\mathrm{t}),\ \nu_2(\mathrm{t})) : (\nu_1(\mathrm{t}),\ \nu_2(\mathrm{t})) \in [0,1] \times [0,1],\ \mathrm{t} \in [0, \mathrm{T}_1]\}.$$

where the control parameters $\nu_1(t),\ \nu_2(t)$ are measurable and bounded function for $t \in [0, \mathrm{T}_1]$. When people take a full violation of precautionary measures (like social distance), then $\nu_1(\mathrm{t})$ takes lowest value which is 0. When people take full maintaining the precautionary measure then $\nu_1(\mathrm{t})$ takes highest value which is 1. In other situation, the control variable is in $\nu_1(\mathrm{t}) \in (0, 1)$. $\nu_2(\mathrm{t})$ represents as control policy which is due to protective measure susceptible population directly moves to recovered population. From beginning it satisfies $0 \le \nu_2(\mathrm{t}) \le 1$.

Theorem 6: In the region $\psi = \{(\nu_1(\mathrm{t}),\ \nu_2(\mathrm{t})) : (\nu_1(\mathrm{t}),\ \nu_2(\mathrm{t})) \in [0,1] \times [0,1],\ \mathrm{t} \in [0, \mathrm{T}_1]\}$ the optimal control intervention $(\nu_1^*,\ \nu_2^*)$ which minimizes L_1 is given by $\nu_1^* = \max\{0, \min(\bar{\nu}_1,\ 1)\}$ and $\nu_2^* = \max\{0, \min(\bar{\nu}_2,\ 1)\}$ where $\bar{\nu}_1 = \frac{(\tau_2 - \tau_1)\lambda SE}{2k_2}$, $\bar{\nu}_2 = \frac{(\tau_1 - \tau_7)S}{2k_3}$.

Proof: The Lagrangian of the problem is given by $L_2 = k_1 I + k_2 {\nu_1}^2 + k_3 {\nu_2}^2$. Let us define the Hamiltonian function as $\tilde{H}(S,\ E,\ Q, A,\ I, M,\ R,\ \nu_1, \nu_2, \tau) = L_2(I,\ \nu_1, \nu_2) + \tau_1 \frac{dS}{dt} + \tau_2 \frac{dE}{dt} + \tau_3 \frac{dQ}{dt} + \tau_4 \frac{dA}{dt} + \tau_5 \frac{dI}{dt} + \tau_6 \frac{dM}{dt} + \tau_7 \frac{dR}{dt}$. Here, $\tau = (\tau_1,\ \tau_2,\ \tau_3,\ \tau_4,\ \tau_5, \tau_6,\ \tau_7)$ are all adjoint variables. According to the maximum principle from Pontryagin et al. (1962), the cost functional may be minimized by the minimized Hamiltonian. We can compute the Hamiltonian by solving the following equations

$$\frac{d\tau_1}{dt} = -\frac{\partial \tilde{H}}{\partial S} = \tau_1\{(1-\nu_1)\lambda E + \beta_1 + d + \nu_2\} - \tau_2(1-\nu_1)\lambda E - \tau_3\beta_1 - \tau_7\nu_2$$

$$\frac{d\tau_2}{dt} = -\frac{\partial \tilde{H}}{\partial E} = \tau_1(1-\nu_1)\lambda S - \tau_2\{(1-\nu_1)\lambda S - (r_1 + \beta_2 + d)\} - \tau_3\beta_2 - \tau_4\gamma_1 - \tau_5 r_1$$

$$\frac{d\tau_3}{dt} = -\frac{\partial \tilde{H}}{\partial Q} = \tau_3(r_2 + \sigma_1 + d) - \tau_5 r_2 - \tau_6 k - \tau_7\sigma_1$$

$$\frac{d\tau_4}{dt} = -\frac{\partial \tilde{H}}{\partial A} = \tau_4(d + \sigma_2) - \tau_7\sigma_2$$

$$\frac{d\tau_5}{dt} = -\frac{\partial \tilde{H}}{\partial I} = -k_1 + \tau_5(\gamma_2 + \sigma_3 + d) - \tau_6\gamma_2 - \tau_7\sigma_3$$

$$\frac{d\tau_6}{dt} = \tau_6(\delta + \sigma_4 + d) - \tau_7\sigma_4$$

$$\frac{d\tau_7}{dt} = \tau_7 d \qquad (12)$$

The differential equation satisfies the transversality conditions $\tau_i(T_1) = 0,\ \ i = 1,\ 2,\ 3,\ 4,\ 5,\ 6,\ 7$. From the optimality conditions, we derive

$\frac{\partial \tilde{H}}{\partial \nu_1} = 0$ and $\frac{\partial \tilde{H}}{\partial \nu_2} = 0$ at the point $\nu_1 = \overline{\nu_1}$ and $\nu_2 = \overline{\nu_2}$, respectively. The variables ν_1 and ν_2 take the following values

$$\nu_1 = \overline{\nu_1} = \frac{(\tau_2 - \tau_1)\lambda SE}{2k_2} \text{ and } \nu_2 = \overline{\nu_2} = \frac{(\tau_1 - \tau_7)S}{2k_3}$$

The lower bound and upper bound of two controls are 0 and 1 respectively. Therefore, we have $\nu_1^* = 0$ if $\overline{\nu_1} < 0$ and $\nu_1^* = 1$ if $\overline{\nu_1} > 1$, otherwise $\nu_1^* = \overline{\nu_1}$. Similar results hold for other control parameter ν_2. Hence, the optimal value of the functional L_1 for the pair of control $(\nu_1^*,\ \nu_2^*)$ is drawn.

6. Numerical Results

In this section, we study the theoretical results and explain through some graphical representation.

Result 1: Let us assume the values of the parameters $\widetilde{\Pi} = (6,\ 8,\ 10\ ),\ \widetilde{\lambda} = (2.8 \times 10^{-5},\ 3.8 \times 10^{-5},\ 4.8 \times 10^{-5})$,

$\widetilde{\beta_1} = (0.35, 0.45, 0.55),\ \widetilde{\beta_2} = (0.1, 0.2, 0.3),\ \widetilde{r_1} = (0.01, 0.02, 0.03),\ \widetilde{r_2} = (0.5, 0.6, 0.7),\ \widetilde{\sigma_1} = (0.005, 0.006, 0.007),\ \widetilde{\sigma_2} = (0.034, 0.044, 0.054),\ \widetilde{\gamma_1} = (0.275, 0.276, 0.277),\ \widetilde{\gamma_2} = (0.44, 0.45, 0.46),\ \widetilde{\sigma_3} = (0.001, 0.0011, 0.0012),\ \widetilde{\sigma_4} = (0.85, 0.86, 0.87),\ \widetilde{k} = (0.95, 0.96, 0.97),\ \widetilde{\delta} = (0.01, 0.02, 0.03),\ \widetilde{d} = (0.97, 0.98, 0.99)$ at $\alpha = 0.1, w_1 = 0.2,\ w_2 = 0.8$.

We choose above hypothetical data of all biological parameters. Figure 2 has been drawn. We have infection free equilibrium point $E_1{}^0 = (6.627, 0, 0, 0, 0, 0, 0)$. Therefore, the system (5) becomes asymptotically stable at $E_1{}^0$.

Figure 2
Population trajectories of infection-free equilibrium point

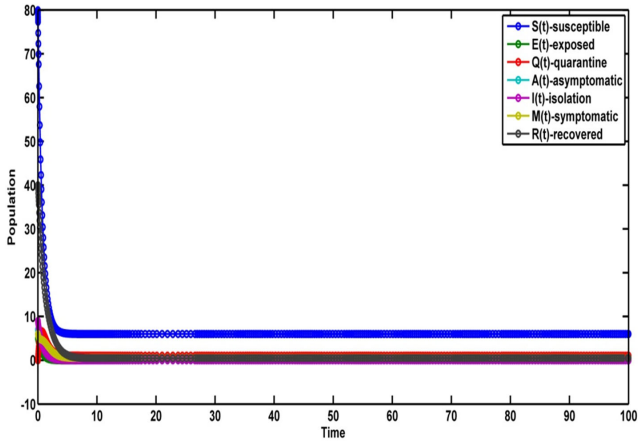

Result 2: Let $\widetilde{\Pi} = (2000000, 2000010, 2000020)$, $\widetilde{\gamma} = (.00000028, .00000038, .00000048)$

$\widetilde{\beta_1} = (0.35, 0.45, 0.55), \widetilde{\beta_2} = (0.1, 0.2, 0.3), \widetilde{r_1} = (0.01, 0.02, 0.03), \widetilde{r_2} = (0.5, 0.6, 0.7), \widetilde{\alpha_3} = (0.001, 0.0011, 0.0012), \widetilde{\alpha_4} = (0.85, 0.86, 0.87), \widetilde{k} = (0.95, 0.96, 0.97), \widetilde{\delta} = (0.01, 0.02, 0.03), \widetilde{d} = (0.17, 0.18, 0.19)$ at $\alpha = 0.1, w_1 = 0.2, w_2 = 0.8$.

It is seen that $\Delta_1 = A_1 > 0$, $\Delta_2 = A_1A_2 - A_3 > 0$, $\Delta_3 = A_1A_2A_3 - A_1{}^2A_4 - A_3{}^2 + A_1A_5 > 0$ $\Delta_4 = A_6A_1{}^2A_2 - A_1{}^2A_4{}^2 - A_1A_2{}^2A_5 + A_1A_2A_3A_4 - A_6A_1A_3 + 2A_1A_4A_5 + A_2A_3A_5 - A_3{}^2A_4 - A_5{}^2 > 0$.

$\Delta_5 = -A_1{}^3A_6{}^2 + 2A_1{}^2A_2A_5A_6 + A_1{}^2A_3A_4A_6 - A_1{}^2A_4{}^2A_5 - A_1A_2{}^2A_5{}^2 - A_1A_2A_3{}^2A_6 + A_1A_2A_3A_4A_5 - 3A_1A_3A_5A_6 + 2A_1A_4A_5{}^2 + A_2A_3A_5{}^2 + A_3{}^3A_6 - A_3{}^2A_4A_5 - A_5{}^3 > 0$.

So, the system (5) is locally asymptotically stable around $E_1{}^*(106795.58, 5878412.65, 894184.78, 6143674.35, 1094051.45, 1242804.36, 36477129.37)$.

Figure 3 represents the population trajectories for the endemic equilibrium points. We consider the above data set for Figure 4 with the help of fixed $\alpha = 0.1$. From these figures, it is seen that the weight w_1 increases and w_2 decreases and then the level of equilibrium of susceptible population increases gradually and recovered population gradually increases (from Figure 4(a), (b)). The rest of the figure indicates this population decreases gradually in the environment. This figure represents that exposed population and asymptomatic population in our environment increase gradually and other population decreases.

We use the above same set of parametric values for Figure 5. With the help of different values of α and fixed values for for $w_1 = 0.3$, $w_2 = 0.7$. Figure 5 has been drawn. In the figure, deep

Figure 3
The population trajectories of endemic equilibrium point

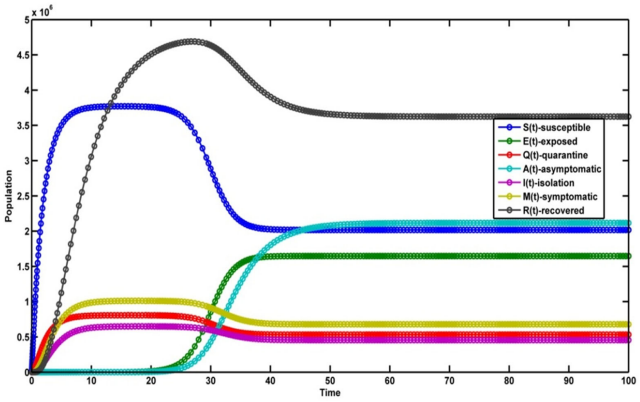

blue line indicates susceptible population, green line indicates exposed population, red line indicates quarantine population, sky blue line indicates asymptomatic population, purple line indicates isolation population, yellow line indicates symptomatic population, and black line indicates recovered population. From these figures, it is concluded that all the population decreases gradually as the value of α increases. It is concluded that all the population of the environment depends on the imprecise biological parameters.

We have taken the fixed $\alpha = 0.1$, $w_1 = 0.5$, $w_2 = 0.5$ for same set of parametric values to draw Figure 6. We plot the phase portrait between different populations. From this figure, it is concluded that all the population is dominated by the imprecise nature of parameter.

We represent the profiles of population for the control variables $v_1 = 0.3, v_2 = 0.0$; $v_1 = 0.0, v_2 = 0.3$; $v_1 = 0.0, v_2 = 0.0$ (without control); $v_1 = 0.3, v_2 = 0.3$ (with control) in Figure 7. For without control variables the susceptible individual is immensely increased in 10–20 days and then suddenly decreased. In these figures, we observe that the susceptible population is highly increased for 20–30 days and then decreased and a fixed line after 40 days for $v_1 = 0.3$, $v_2 = 0.0$. The susceptible population is maximum between 5 and 15 days for $v_1 = 0.0, v_2 = 0.3$ and then gradually decreases. For with control variables, the population is maximum in 5 days and it is fixed line between 5 days to 55 days and then gradually decreases. So the susceptible individual is greatly influenced by the change of control variables. For without control variables, the exposed population is progressively increased and it is a fixed line after 30 days. From the figure, it is seen that the exposed population is gradually increased and it is a fixed line after 40 days. We have a significant change for $v_1 = 0.3, v_2 = 0.0$ and $v_1 = 0.0$, $v_2 = 0.3$. If both control variables are applied, then the population is gradually increased after 50 days. For without control variables, the quarantine population is highly increased in 10–20 days and with control variables it is less increase than without control variables. We have shown that a significant change for exposed population and asymptomatic population can be arisen for the change of control variables. A meaningful change is observed between isolated and symptomatic population for the variation of control variables. For the effect of without control and with control, we have seen that the recovered population is less enough between them. The recovered population is a fixed line from 20 days to 55 days and then slightly decreased using control variables $v_1 = 0.3, v_2 = 0.3$. A significant deflection is shown for $v_1 = 0.3, v_2 = 0.0$ and $v_1 = 0.0, v_2 = 0.3$.

Figure 4
Population trajectories for different values of w_1 and w_2 and fixed value of $\alpha = 0.1$

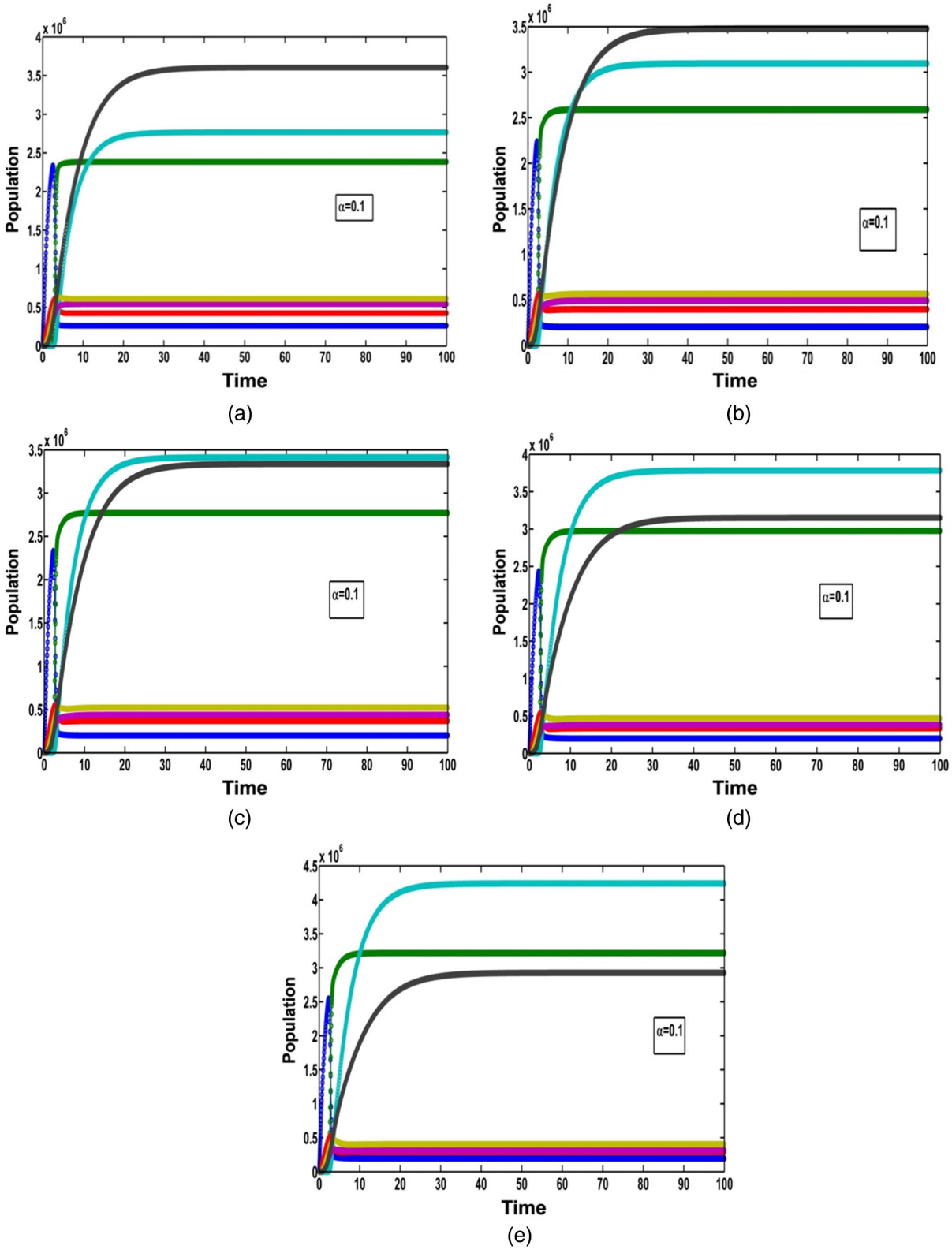

Figure 5
Population trajectories for different values of α

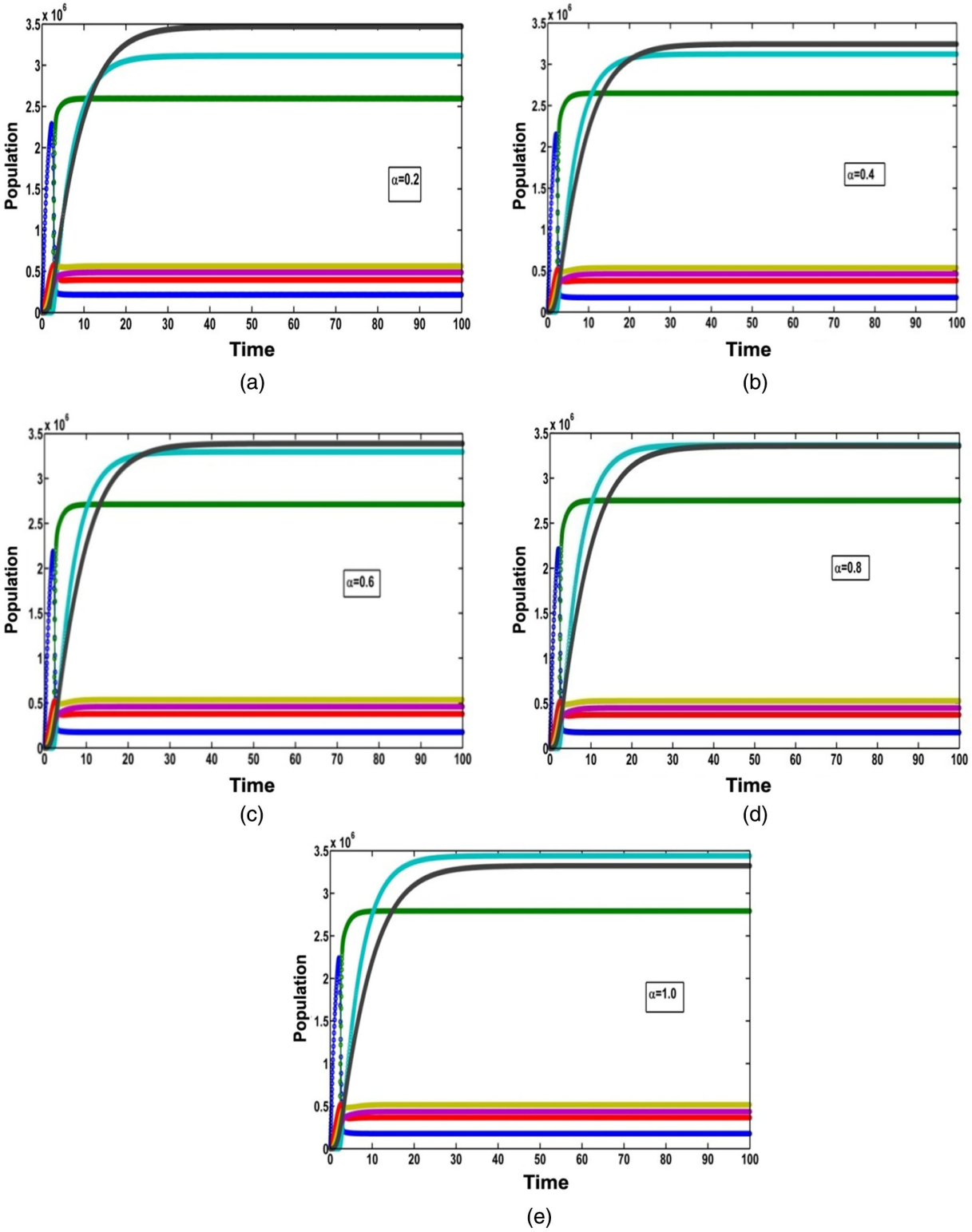

Figure 6

Plotting of phase portrait for $\alpha = 0.1$ and $w_1 = 0.5,\ \ w_2 = 0.5$ (a) susceptible versus exposed, (b) susceptible versus symptomatic, (c) susceptible versus recovered, (d) quarantine versus isolated, (e) asymptomatic versus symptomatic, (f) exposed versus recovered, (g) quarantine versus recovered, and (h) symptomatic versus recovered

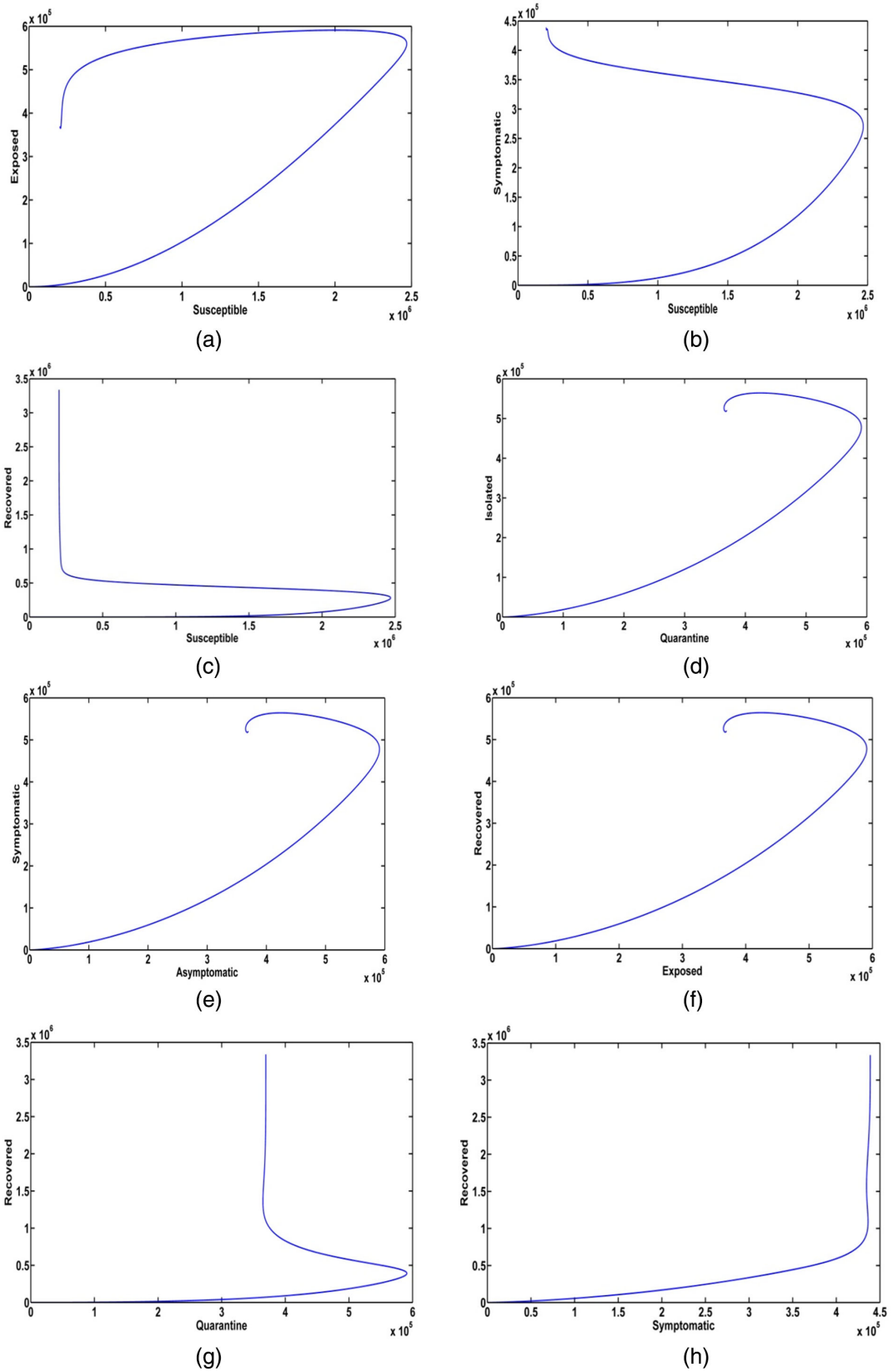

Figure 7
Population trajectories with both control and without control variables

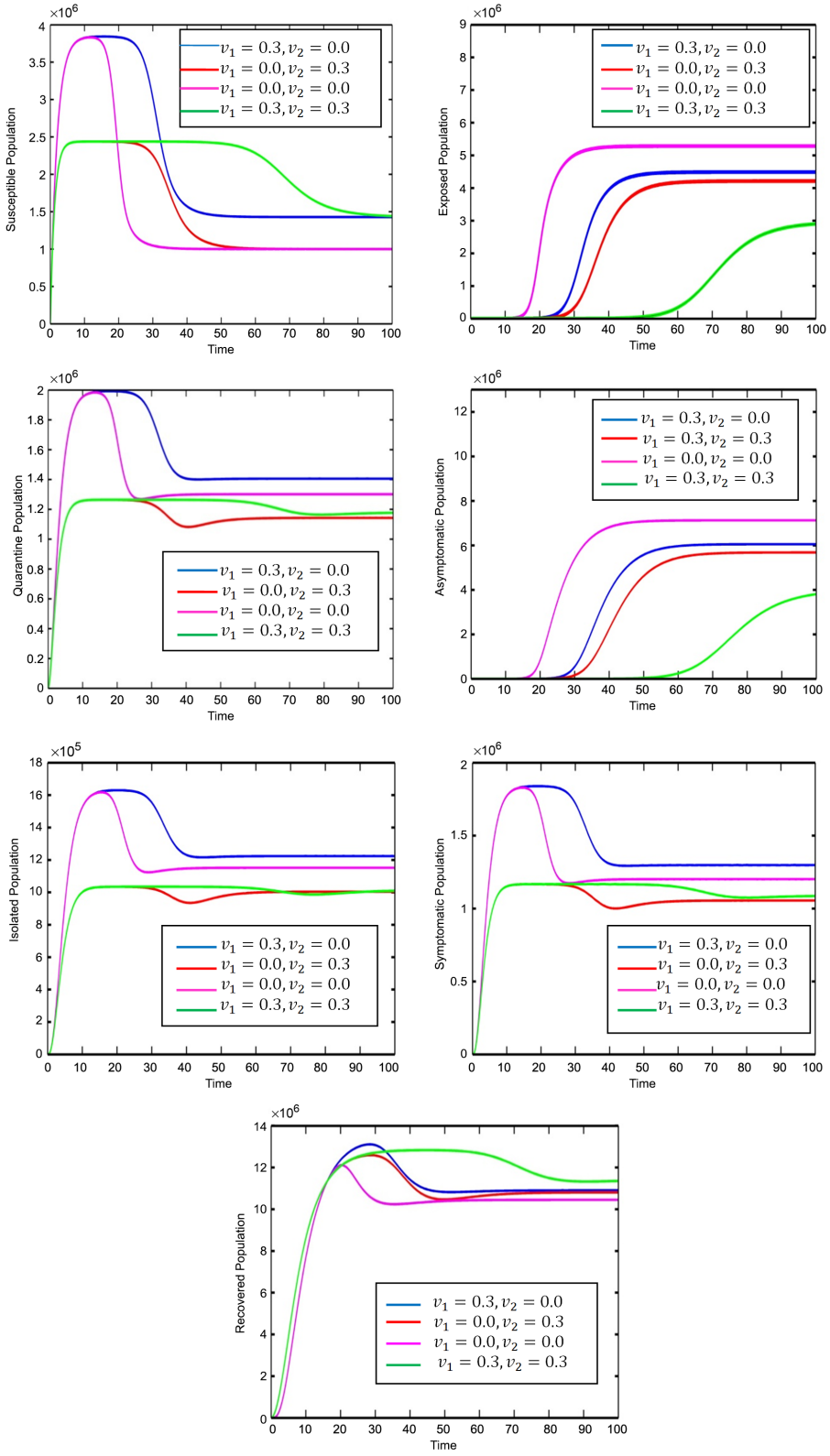

7. Conclusions

During this pandemic situation, prediction mathematical model is the most important tool for sketching the technique to control coronavirus disease. In this article, we have analyzed a newly developed epidemic SEQAIMR model. In the fuzzy model, all the biological parameters considered as imprecise parameters due to natural disaster (like earthquake, flood, wildfires, etc.) and human activity (like financial crisis) change continuously the value of the parameters. Assuming the total population is divided into seven subpopulations such as susceptible, exposed, quarantine, asymptomatic, symptomatic, isolation, recovered. We have explained the stability analysis of the fuzzy coronavirus disease model. We have determined the basic reproduction number (R_0) (Diekmann et al., 1990). We have described that the infection-free equilibrium of the system will be locally asymptotically stable and globally asymptotically stable for $R_0 < 1$. The global asymptotically stability around the endemic equilibrium point has been analyzed in our work. All biological parameters are treated as imprecise nature. We have performed the infection-free equilibrium and endemic equilibrium point by graphical representation in our numerical simulation part. The figures are drawn for fixed value α. The significant change of the population trajectories is shown for weighted w_1, w_2. From this figure, we have concluded that imprecise biological parameters can affect the population. Lastly population trajectories with control and without control are adopted by graphically representation. The disease load can be condensed by control interventions. Therefore, we hope that our model can be used to develop the biological field. One may improve the epidemic model with the use of stochastic, fuzzy and intuitionistic fuzzy uncertainty.

Acknowledgements

The authors are thankful to the respected editors and anonymous reviewers for their constructive comments and suggestions for the improvement of the article.

Funding Support

The first author would like to acknowledge the financial support provided by DST-INSPIRE, Government of India, Ministry of Science & Technology, New Delhi, India (DST/INSPIRE Fellowship/2017/IF170211).

Conflicts of Interest

The authors declare that they have no conflicts of interest to this work.

Data Availability Statement

Data sharing is not applicable to this article as no new data were created or analyzed in this study.

References

Buonomo, B., d'Onofrio, A., & Lacitignola, D. (2008). Global stability of an SIR epidemic model with information dependent vaccination. *Mathematical Bioscience*, *216*(1), 9–16. https://doi.org/10.1016/j.mbs.2008.07.011

Cai, Y., Kang, Y., & Wang, W. (2017). A stochastic SIRS epidemic model with nonlinear incidence rate. *Applied Mathematics and Computation*, *305,* 221–240. https://doi.org/10.1016/j.amc.2017.02.003

Castillo-Chavez, C., & Song, B. (2004). Dynamical models of tuberculosis and their applications. *Mathematical Bioscience and Engineering*, *1*(2), 361–404. https://doi.org/10.3934/mbe.2004.1.361

Chakraborty, T., & Ghosh, I. (2020). Real-time forecasts and risk assessment of novel coronavirus (COVID-19) cases: A data-driven analysis. *Chaos Soliton & Fractal*, *135*, 109850. https://doi.org/10.1016/j.chaos.2020.109850

Chang, Z., Meng, X., & Lu, X. (2017). Analysis of a novel stochastic SIRS epidemic model with two different saturated incidence rates. *Physica A: Statical Mechanics and Its Application*, *472*, 103–116. https://doi.org/10.1016/j.physa.2017.01.015

Chen, Y., Liu, Q., & Guo, D. (2020). Emerging coronaviruses: Genome structure, replication, and pathogenesis. *Journal of Medical Virology*, *92*(4), 418–423. https://doi.org/10.1002/jmv.26234

Das, S., Mahato, P., Mahato, S. K., & Pal, D. (2022). A mathematical study of pandemic COVID-19 virus with special emphasis on uncertain environments. *Journal of Applied Nonlinear Dynamics 11*(2), 427–457. https://doi.org/10.5890/JAND.2022.06.012

Diekmann, O., Heesterbeek, J. A. P., & Metz, J. A. J. (1990). On the definition and the computation of the basic reproduction ratio *R*0 in models for infectious diseases in heterogeneous populations. *Journal of Mathematical Biology*, *28*(4), 365–382. https://doi.org/10.1007/BF00178324

Giordano, G., Blanchini, F., Bruno, R., Colaneri, P., Filippo, A. D., Matteo, A. D., & Colaneri, M. (2020). Modelling the COVID-19 epidemic and implementation of population-wide interventions in Italy. *Nature Medicine*, *26*(6), 855–860. https://doi.org/10.1038/s41591-020-0883-7

He, X., Lau, E. H., Wu, P., Deng, X., Wang, J., Hao, X., . . . , & Leung, G. M. (2020). Temporal dynamics in viral shedding and transmissibility of COVID-19. *Nature Medicine*, *26*(5), 672–675. https://doi.org/10.1038/s41591-020-0869-5

Imai, N., Cori, A., Dorigatti, I., Baguelin, M., Donnelly, C. A., Riley, S. & Ferguson, N. M. (2020). Transmissibility of 2019-nCoV. *Imperial College London*, 1–6. https://doi.org/10.25561/77148

Kampf, G., Todt, D., Pfaender, S., & Steinmann, E. (2020). Persistence of coronaviruses on inanimate surfaces and their inactivation with biocidal agents. *Journal of Hospital Infection, 104*(3), 246–251. https://doi.org/10.1016/j.jhin.2020.01.022

Khajanchi, S., & Sarkar, K. (2020). Forecasting the daily and cumulative number of cases for the COVID-19 pandemic in India. *Chaos*, *30*(7), 071101. https://doi.org/10.1063/5.0016240

Khajanchi, S., Sarkar, K., & Mondal, J. (2020). Dynamics of the COVID-19 pandemic in India. *arXiv Preprint: 2005.06286.*

Kumar, S., Sharma, S., & Kumari, N. (2020). Future of COVID-19 in Italy: A mathematical perspective. *arXiv Preprint: 2004.08588.*

Lahrouz, A., Omari, L., & Kiouach, D. (2011). Global analysis of a deterministic and stochastic nonlinear SIRS epidemic model. *Nonlinear Analysis: Modelling and Control*, *16*(1), 59–76. https://doi.org/10.15388/NA.16.1.14115

Liang, K. (2020). Mathematical model of infection kinetics and its analysis for COVID-19, SARS and MERS. *Infection, Genetics and Evolution, 82*, 104306 https://doi.org/10.1016/j.meegid.2020.104306

Mahato, P., Das, S., & Mahato, S. K. (2022). An epidemic model through information-induced vaccination and treatment under fuzzy impreciseness. *Modeling Earth Systems and Environment*, *8*(3), 2863–2887. https://doi.org/10.1007/s40808-021-01257-7

Mondal, P. K., Jana, S., Haldar, P., Kar, T. K. (2015). Dynamical behaviour of an epidemic model in a fuzzy transmission. *International Journal of Uncertainity, Fuzziness and Knowledge-Based Systems, 23*(5), 651–665. https://doi.org/10.1142/S0218488515500282

Nadim, S. S., Ghosh, I., & Chattopadhyay, J. (2021). Short-term predictions and prevention strategies for COVID-2019: A model based study. *Applied Mathematics and Computation*, *404*, 126251. https://doi.org/10.1016/j.amc.2021.126251.

Nandi, S. K., Jana, S., Manadal, M., & Kar, T. K. (2018). Analysis of a fuzzy epidemic model with saturated treatment and disease transmission. *International Journal of Biomathematics*, *11*(1), 1850002. https://doi.org/10.1142/S179352451850002X

Nesteruk, I. (2020). Long term prediction for COVID-19 pandemic dynamics in Ukraine, Austria and Italy. *medRxiv Preprint*. https://doi.org/10.1101/2020.04.08.20058123

Pal, D., Ghosh, D., Santra, P. K., & Mahapatra, G. S. (2020). Mathematical analysis of a COVID-19 epidemic model by using data driven epidemiological parameters of diseases spread in India. *medRxiv Preprint.* https://doi.Org/10.1101/2020.04.25.20079111

Panja, P., Mondal, S. K., & Chattopadhyay, J. (2017). Dynamical study in fuzzy threshold dynamics of a cholera epidemic model. *Fuzzy Information and Engineering, 9*(3), 381–401. https://doi.org/10.1016/j.fiae.2017.10.001

Pontryagin, L. S., Boltyanskii, V. G., Gamkrelidze, R. V., & Mishchenko, E. F. (1962). *The Mathematical Theory of Optimal Processes.* USA: Wiley.

Read, J. M., Bridgen, J., Cummings, D. A. T., Ho, A., & Jewell, C. P. (2021). Novel coronavirus 2019-nCoV (COVID-19): Early estimation of epidemiological parameters and epidemic size estimates. *Philosophical Transactions of the Royal Society B: Biological Sciences*, *376*(1829), 20200265. https://doi.org/10.1098/rstb.2020.0265

Senapati, A., Rana, S., Das, T., & Chottopadhyay, J. (2021). Impact of intervention on the spread of COVID-19 in India: A model based study. *Journal of Theoretical Biology*, *523*, 110711. https://doi.org/10.1016/j.jtbi.2021.110711

Tiwari, A. (2020). Modelling and analysis of COVID-19 epidemic in India. *Journal of Safety Science and Resilience*, *1*(2), 135–140. https://doi.org/10.1016/j.jnlssr.2020.11.005

van den Driessche, P., & Watmough, J. (2002). Reproduction numbers and sub-threshold endemic equilibria for compartmental models of disease transmission. *Mathematical Biosciences*, *180*(1-2), 29–48. https://doi.org/10.1016/S0025-5564(02)00108-6

Velavan, T. P., & Meyer, C. G. (2020). The COVID-19 epidemic. *Tropical Medicine & International Health*, *25*(3), 278–280. https://doi.org/10.1111/tmi.13383

Verity, R., Okell, L. C., Dorigatti, I., Winskill, P., Whittaker, C., Imai, N., . . . , & Ferguson, N. M. (2020). Estimates of the severity of coronavirus disease 2019: A model-based analysis. *The Lancet Infectious Diseases*, *20*(6), 669–677. https://doi.org/10.1016/S1473-3099(20)30243-7

Verma, R., Tiwari, S. P., & Upadhyay, R. K. (2019). Transmission dynamics of epidemic spread and outbreak of Ebola in West Africa: Fuzzy modeling and simulation. *Journal of Applied Mathematics and Computing*, *60*(1), 637–671. https://doi.org/10.1007/s12190-018-01231-0

Volpert, V., Banerjee, M., & Petrovskii, S. (2020). On a quarantine model of coronavirus infection and data analysis. *Mathematical Modelling of Natural Phenomena*, *15*, 24. https://doi.org/10.1051/mmnp/2020006

Wu, J. T., Leung, K., & Leung, G. M. (2020). Nowcasting and forecasting the potential domestic and international spread of the 2019-ncov outbreak originating in Wuhan, China: A modelling study. *The Lancet*, *395*(10225), 689–697. https://doi.org/10.1016/S0140-6736(20)30260-9

Wu, Z., & McGoogan, J. M. (2020). Characteristics of and important lessons from the coronavirus disease 2019 (COVID-19) outbreak in China: Summary of a report of 72,314 cases from the Chinese Center for Disease Control and Prevention. *Journal of American Medical Association*, *323*(13), 1239–1242. https://doi.org/10.1001/jama.2020.2648

Yang, C., & Wang, J. (2020). A mathematical model for the novel coronavirus epidemic in Wuhan, China. *Mathematical Biosciences and Engineering, 17*(3), 2708–2724. https://doi.org/10.3934%2Fmbe.2020148

Zadeh, L. A. (1965). Fuzzy sets. *Information and Control*, *8*(3), 338–353. https://doi.org/10.1016/s0019-9958(65)90241-x

How to Cite: Mahato, P., Mahato, S. K., & Das, S. (2024). COVID-19 Outbreak with Fuzzy Uncertainties: A Mathematical Perspective. *Journal of Computational and Cognitive Engineering*, *3*(1), 43–57. https://doi.org/10.47852/bonviewJCCE2202236